THE JOURNAL OF BIOLOGICAL CHEMISTRY VOL. 285, NO. 35, pp. 26916–26922, August 27, 2010

Defining Specific Lipid Binding Sites for a Peripheral Membrane Protein *in Situ* Using Subtesla Field-cycling NMR*[S]

Received for publication, March 12, 2010, and in revised form, June 21, 2010 Published, JBC Papers in Press, June 24, 2010, DOI 10.1074/jbc.M110.123083

Mingming Pu[‡], Andrew Orr[‡], Alfred G. Redfield[§], and Mary F. Roberts[‡1]

From the [‡]Department of Chemistry, Boston College, Chestnut Hill, Massachusetts 02465 and the [§]Department of Biochemistry, Brandeis University, Waltham, Massachusetts 024547

Despite the profound physiological consequences associated with peripheral membrane protein localization, only a rudimentary understanding of the interactions of proteins with membrane surfaces exists because these questions are inaccessible by commonly used structural techniques. Here, we combine high resolution field-cycling ^{31}P NMR relaxation methods with spin-labeled proteins to delineate specific interactions of a bacterial phospholipase C with phospholipid vesicles. Unexpectedly, discrete binding sites for both a substrate analogue and a different phospholipid (phosphatidylcholine) known to activate the enzyme are observed. The lifetimes for the occupation of these sites (when the protein is anchored transiently to the membrane) are >1–2 μs (but <1 ms), which represents the first estimate of an off-rate for a lipid dissociating from a specific site on the protein and returning to the bilayer. Furthermore, analyses of the spin-label induced NMR relaxation corroborates the presence of a discrete tyrosine-rich phosphatidylcholine binding site whose location is consistent with that suggested by modeling studies. The methodology illustrated here may be extended to a wide range of peripheral membrane proteins.

Transient interactions of peripheral membrane proteins with bilayers play critical roles in signal transduction cascades. Many of these proteins are proposed to have binding interactions with multiple distinct types of phospholipids (now usually characterized by bulk protein binding with different lipid components and mutagenesis to see whether suspected regions on the protein are correlated with higher affinity binding of the protein). Confirming whether there is a discrete site, whether a lipid binds, and with what affinity, when the protein interacts with a multicomponent bilayer is difficult at best. Nonspecific interactions with the bilayer also can occur. Conformation of the bound macromolecule also is hard to deduce, particularly if the affinity of the protein for the interface is of only moderate affinity (a trait desirable in many peripheral proteins if they are to bind and dissociate from the membrane repeatedly). These proteins often have flexible loops or domains that are likely to be affected by membrane binding. Methods that can address whether and where specific phospholipid sites exist on a peripheral protein when anchored to a bilayer would aid in understanding how its function may be modulated.

An interesting case is the secreted phosphatidylinositol-specific phospholipase C (PI-PLC)[2] from *Bacillus thuringiensis.* This small (35 kDa) enzyme is a good model for the catalytic domain of the human PI-PLC. It specifically catalyzes the cleavage of PI to form diacylglycerol and inositol 1-phosphate. Crystal structures of this protein show a monomeric αβ-barrel (1). Anionic phospholipids such as phosphatidylmethanol (PMe) are competitive inhibitors and can therefore serve as substrate analogues (2). PI-PLC is activated specifically by phosphatidylcholine (PC) present in the interface (2–4); the PC aids in vesicle binding (5), and it also increases k_{cat}. Although this observation might suggest that PI-PLC contains an activator binding site, it has been impossible to demonstrate the presence of a discrete site on the protein.

Here, we combine spin-label relaxation methods with high resolution field-cycling NMR (6, 7) to investigate the membrane interactions of this PI-PLC. These elements have been used previously, but here, they are combined to provide unique insights into protein/phospholipid interactions. Our method uses the high field of a superconducting magnet to prepare the nuclear spins and to allow us to follow ^{31}P resonances for multiple phospholipid headgroups in the same vesicle. The sample is shuttled to the low field region of the bore of the magnet, where the spins relax (8). The sample is returned to high field, where the relaxation of each nuclear species (in this case, both PC and PMe in the same vesicle) can be monitored. The presence of a spin-label increases ^{31}P nuclear relaxation in a distance-dependent manner, so that the location of the lipid binding site(s) can be mapped by attaching a spin-label to different positions on PI-PLC (Fig. 1). Using this method, we can identify distinct substrate and activator binding sites as well as begin to map out how the protein is anchored transiently to the membrane.

EXPERIMENTAL PROCEDURES

Chemicals—The spin-label reagent 1-oxyl-2,2,5,5-tetramethylpyrroline-3-methyl-methanethio-sulfonate was obtained from Toronto Research Chemicals, Inc. 1-Palmitoyl-2-oleoyl-phosphatidylcholine and dioleoylphosphatidylmethanol, from

* This work was supported, in whole or in part, by National Institutes of Health Grants GM60418 (to M. F. R.) and GM077974 (to A. G. R.). This work was also supported by National Science Foundation Grant MCB-0517381 (to M. F. R.).

[S] The on-line version of this article (available at http://www.jbc.org) contains supplemental "Experimental Procedures" and Figs. S1–S4.

[1] To whom correspondence should be addressed: Merkert Chemistry Center, 2609 Beacon St., Chestnut Hill, MA 02467. Fax: 617-552-2705; E-mail: mary.roberts@bc.edu.

[2] The abbreviations used are: PI-PLC, phosphatidylinositol-specific phospholipase C; PC, phosphatidylcholine; SUV, small unilamellar vesicle; PRE, paramagnetic relaxation enhancement; T, tesla; diC$_4$PC, dibutyroyl-PC; diC$_6$PC, dihexanoyl-PC.

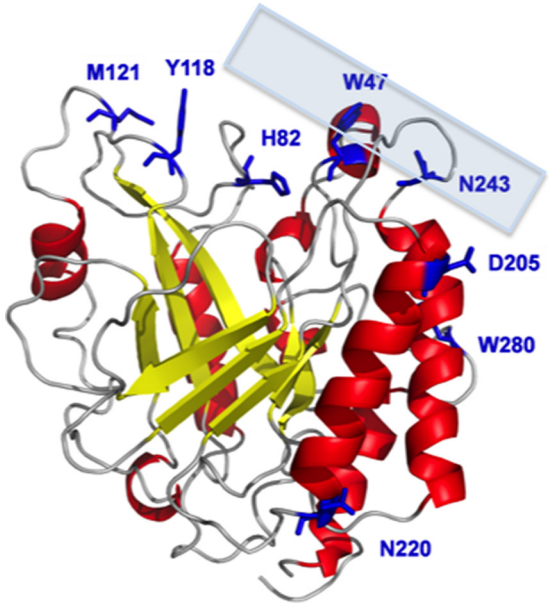

FIGURE 1. **PI-PLC structure (Protein Data Bank code 1PTD).** Residues colored in *blue* show positions where a spin-label was introduced. The *semitransparent box* provides a rough idea of the orientation of the protein with respect to the membrane based on Trp^{47} and Trp^{242} partitioning into the membrane.

Avanti Polar Lipids, Inc., were used without further purification. D_2O was purchased from Sigma. All other chemicals were reagent grade.

PI-PLC Mutations and Spin-labeling—Cys mutations (to generate W47C, H82C, Y118C, M121C, D205C, N220C, N243C, and W280C) of the *B. thuringiensis* PI-PLC gene were constructed by QuikChange methodology (Stratagene) following specific instructions described previously (9). Details of overexpression and purification of the recombinant proteins also have been described (9). Typically, this procedure yielded > 95% pure PI-PLC as monitored by SDS-PAGE. Protein concentrations were estimated by A_{280} and the calculated extinction coefficient based on the sequence. Prior to spin-labeling, the purified PI-PLC variants (5 mg/ml in 20 mM Tris, pH 8.0) were first incubated with 3-fold dithiothreitol at room temperature for 20 min for full reduction of any intermolecular disulfide bonds. A 10-fold excess of the spin-label reagent was then added. The mixture was incubated for 1 h at room temperature and then overnight at 4 °C. The excess spin-labeled reagent was removed by elution from Bio-Spin 6 columns (Bio-Rad); at least two and often three columns were used to remove the free spin-label.

Specific activities of proteins with reduced cysteine mutations were within a factor of two of the wild type enzyme specific activity in a PI/diC_7PC assay system (9), with the exception of H82C, which was inactive, as expected for removal of the general acid in the cleavage mechanism. Derivatization with the nitroxide had negligible effects on enzyme-specific activities. Mutants with about half of the control activity (1630 μmol min^{-1} mg^{-1}) included W47C, Y118C, and N243C.

Preparation of Small Unilamellar Vesicles—This bacterial PI-PLC binds well to small unilamellar vesicles (SUVs) but not large vesicles, so that SUVs of PC/PMe were prepared by sonication (5). Samples for use in field cycling were prepared in 8-mm NMR tubes (1-ml volume containing 14.4 μM PI-PLC and PC/PMe (5:5 mM) SUVs in 50 mM HEPES, 1 mM EDTA, pH 7.5), and sealed as described (8) to inhibit bubbles.

High Resolution Field-cycling ^{31}P-NMR—The equipment used for resolution field cycling described previously (8) was modified using a stepper motor drive instead of a pneumatic drive[3] and an extra coil above the superconducting magnet to reach fields below 0.05 T (7). The spin-lattice relaxation rate, $R_1 = 1/T_1$, for the ^{31}P resonances of each phospholipid in the mixed vesicles, was measured as described previously (6, 7) in the absence and presence of different spin-labeled PI-PLC proteins.

Field cycling is limited seriously by the long time scale (0.2–0.5 s) of the shuttling process (8). However, this limitation is offset by the stronger effects observed at very low fields (10) and by optimization of the relative concentrations of spin-labeled PI-PLC and vesicles. In the present experiments, the ^{31}P resonances of the substrate analogue PMe and the activator PC are well separated, so that we can study relaxation behavior of both components of the bilayer in a single experiment with one-dimensional methods.

Modeling Using AutoDock4—The coordinates of ligand butylphosphocholine were generated by CORINA (Molecular Networks). The docking of butylphosphocholine into monomeric PI-PLC (Protein Data Bank code 1PTD) was performed with the program AutoDock4 (11, 12). For docking of the same molecule to a PI-PLC dimer, the structure of W47A/W242A (Protein Data Bank code 2OR2) was used. Its graphical front-end, AutoDockTools, was used to add polar hydrogens and partial charges for protein and ligand. Flexible torsions in the ligands were assigned with the AutoTors module, and all dihedral angles were allowed to rotate freely. Affinity grid fields were generated using AutoGrid4. The genetic algorithm-local search hybrid was used to perform an automated molecular docking. Default parameters were used, except for the number of energy evaluations, which was set to 2,500,000. The lowest docking energy conformations were considered to be the most stable orientations.

RESULTS AND DISCUSSION

Effects of Spin-labeled PI-PLC on ^{31}P Relaxation of PC/PMe Vesicles—We discovered previously that ^{31}P resonances of phospholipids in vesicles have an easily observable relaxation dispersion at low field (<0.01 T) due to interactions with a few nearby protons, with a correlation time ~1 μs. This time reflects overall tumbling of these 250–300-Å diameter vesicles (7). When a spin-labeled enzyme is added (at a concentration of 0.014 mM, much lower than that of the phospholipids in the vesicles, which are 5 mM each), the membrane NMR properties of the lipid ^{31}P resonance at high field are not noticeably perturbed by the spin-label. In contrast, at low field, a dramatic increase in the amplitude of this dispersion can be observed for PMe (Fig. 2*A*) when the spin-label is near the active site (*e.g.* spin-labeled W47C). Such an enhancement is commonly termed paramagnetic relaxation enhancement (PRE) and usually is measured via increases in line width (which is difficult to do and interpret for phospholipids in vesicles because the initial line

[3] A. G. Redfield, unpublished data.

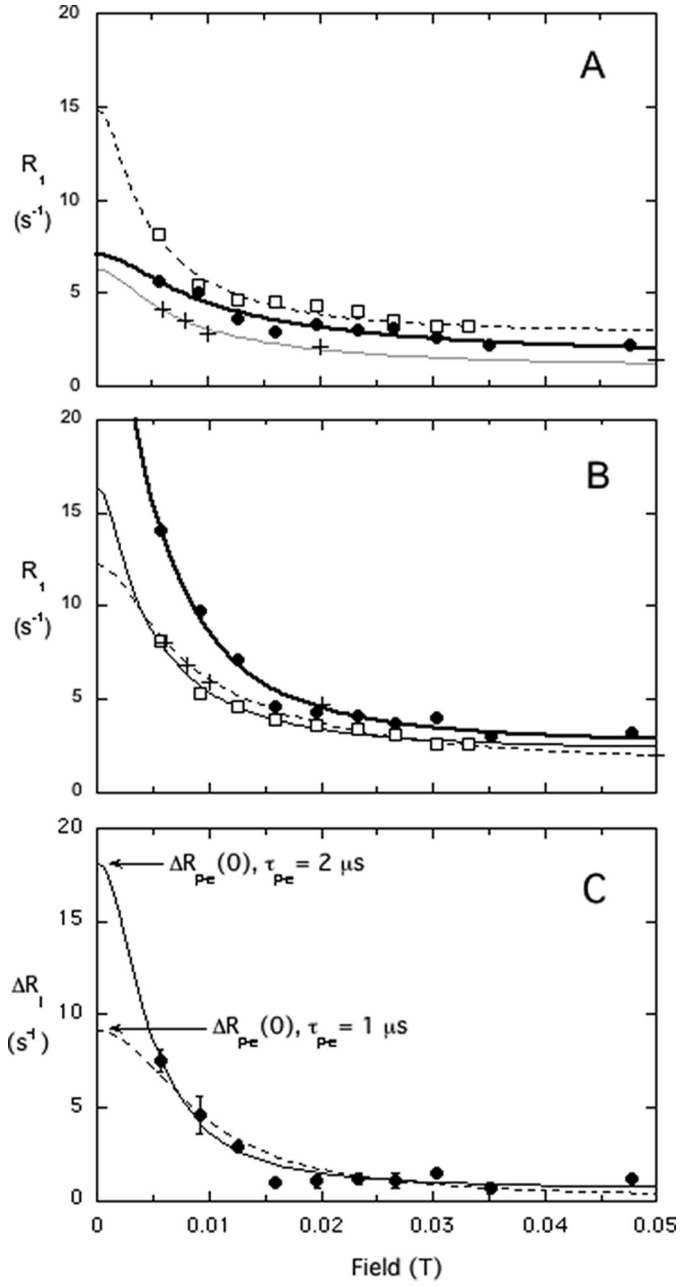

FIGURE 2. Shown is the variation of the ^{31}P R_1 of PMe (*A*) or PC (*B*) with field for mixed vesicles of PC/PMe (5:5 mM) in the presence of 14.4 μM PI-PLC spin-labeled on the cysteine: W47C (□), D205C (●), and N220C (+). *C*, field dependence of the additional PC R_1 component due to spin-labeled D205C protein (ΔR_1). The globally optimized fit (*solid line*) is consistent with $\tau_{P\text{-}e} = 2$ μs; $\Delta R_{P\text{-}e}(0)$, the other key parameter for determining the P-e distance is indicated. If one refits the data in *C* to Equation 1 with a $\tau_{P\text{-}e}$ of 1 μs (shown as a *dotted line*), the $\Delta R_{P\text{-}e}(0)$ is about half of that obtained from using 2 μs; hence, the $\tau_{P\text{-}e}/\Delta R_{P\text{-}e}(0)$ is about the same, leading to the same distance estimate. *Error bars* in *C* are from the least squares fit used to determine R_1 at each field.

widths are 50–70 Hz depending on vesicle size). Importantly, the magnitude of this low field effect varies with the position of the spin-label on PI-PLC, as well as with the ratio of protein to phospholipid (see supplement and Fig. S1 data). Increases in amplitudes also are observed on the dispersion of PC with some of the spin-labeled enzymes (Fig. 2*B*), providing the first evidence that the activator binds to a defined site on the enzyme.

The various spin-labeled enzymes have different PRE effects on the dispersions of PMe and PC (Fig. 2). For example, the spin-label at W47C produces more potent relaxation than that at D205C for PMe (Fig. 2*A*), whereas the spin-labeled D205C is much more potent for PC (Fig. 2*B*). These observations indicate that PI-PLC has separate binding sites for substrates and activators. The results can be analyzed because at low field the chemical shift anisotropy is negligible compared with dipolar interactions.

Strikingly, the horizontal width in field of these two plots (Fig. 2) is similar, suggesting that both PMe and PC dissociate from the enzyme on a much longer time scale than vesicle rotation (~ 1 μs). For PMe, the value of k_{off} must be less than $1/\tau_v = 10^6$ s^{-1} but greater than 2.5×10^3 s^{-1} (the highest observed spin-label rate enhancement, ~10 s^{-1}, multiplied by [lipid]/[enzyme] = 250 (for each lipid in the outer leaflet). Single molecule fluorescence studies[4] with a fluorescently labeled PI-PLC (5) binding to tethered phosphatidylglycerol/PC (1:1) SUVs indicate an average lifetime of the protein on these vesicles as 510 ± 50 ms; this corresponds to a k_{off} of 2.0 ± 0.2 s^{-1}. Thus, the "k_{off}" estimated by these NMR experiments monitors the much shorter dissociation of phospholipid from an enzyme site back into a bilayer with the protein still associated with the bilayer.

Estimating $r_{P\text{-}e}$, the Distance between the Spin-label and a Specific Bound Phospholipid—The ^{31}P PRE data also provide information about the distance between ^{31}P and the spin-labels (6, 7). As opposed to line width changes for phospholipids in bilayers, the changes in R_1 are much easier to interpret as long as one has a full field dependence and understanding of where dipolar relaxation occurs and the correlation time associated with it. The dependence of ΔR_1, the specific enhancement in R_1 caused by the spin-label, on field strength can be described by Equation 1.

$$\Delta R_1 = \Delta R_{P\text{-}e}(0)/(1 + \omega_P^2 \tau_{P\text{-}e}^2) \qquad \text{(Eq. 1)}$$

The contribution of internal motions of the phospholipid and fast motions of the spin-label are expected to be negligibly small. Such motions will contribute only a broad low field dispersion and are observed only in a small baseline shift at fields <0.05 T. We assume that the order parameter $S^2 = 1$ and keep only the term involving the ^{31}P frequency ω_P (the other two possible terms in the full equation are small and may be neglected due to terms with $(\omega_P \pm \omega_e)$, which is dominated by the electron spin frequency ω_e, in the denominators). $\Delta R_{P\text{-}e}(0)$ is the limiting relaxation at zero field, and $\tau_{P\text{-}e}$ is the correlation time for this interaction.

The PRE profile for PC with spin-labeled D205C, generated from data in Fig. 2*B*, is shown in Fig. 2*C*. The shuttling device is not fast enough to measure rates >15 s^{-1}, and we have not made measurements closer to zero field. Nevertheless, the data can be extrapolated assuming a single Lorentzian component to yield a distance of the bound PC to the spin-labeled site on the protein. The correlation time deduced from the fit is ~2 μs and is consistent with the overall tumbling of 250–300-Å diameter vesicles. Assuming a single binding site for a phospholipid, the parameter $\Delta R_{P\text{-}e}(0)$ is proportional to the inverse sixth

[4] M. Pu, A. Gershenson, and M. F. Roberts, unpublished results.

TABLE 1

$\Delta R_{P\text{-}e}(0)$ and extrapolated distances of the phospholipid ^{31}P to spin-label sites ($r_{P\text{-}e}$) using a 2-μs $\tau_{P\text{-}e}$

Samples were for SUVs of 5 mM PC/5 mM PMe with 14.4 μM PI-PLC added. In estimating distances, we assume that for the average size of these SUVs, two-thirds of the total lipid is in the outer monolayer and affected by the spin-label.

PI-PLC	$\Delta R_{P\text{-}e}(0)$		$r_{P\text{-}e}$[a]	
	^{31}PC	^{31}PMe	^{31}PC	^{31}PMe
	s^{-1}		Å	
W47C	3.1 ± 0.7	5.6 ± 0.8	18.0 ± 0.7	16.3 ± 0.4
H82C	5.3 ± 1.0	9.2 ± 0.9	16.4 ± 0.5	15.0 ± 0.2
Y118C	4.1 ± 2.6	0	20.3 ± 2.2	>30
M121C	0	0	>30	>30
D205C	17.6 ± 1.2	2.1 ± 1.0	13.5 ± 0.2	19.2 ± 1.7
N220C	0.2	0.16	28 ± 3	30 ± 4
N243C	4.7 ± 1.3	0.7 ± 0.4	16.8 ± 0.8	23.0 ± 2.6
W280C	3.0 ± 1.5	2.2 ± 0.7	18.1 ± 1.7	19.0 ± 1.0

[a] The errors in $r_{P\text{-}e}$ are estimated using a fixed $\tau_{P\text{-}e}$, but looking at the range for the distance using the maximum and minimum $\Delta R_{P\text{-}e}$. For comparison, the values for spin-labeled W47C (different batches) at three different protein concentrations (0.25, 0.5, and 1 mg/ml) lead to 17.8 ± 1.3 Å for PC and 16.2 ± 1.0 Å for PMe.

power of the distance between the ^{31}P and spin-label ($r_{P\text{-}e}$) according to Equation 2 (6, 7).

$$r_{P\text{-}e}^{6} = ([\text{PI-PLC}]_o/(2/3)[\text{lipid}]_o) \times (S^2\tau_{P\text{-}e}/\Delta R_{P\text{-}e}(0))(0.3\ \mu^2(h/2\pi)^2\gamma_P^2\gamma_e^2) \quad \text{(Eq. 2)}$$

Note that for this size SUV, about two-thirds of the phospholipid is in the outer leaflet.

Although this procedure is approximate, the r^6 dependence means errors in $\tau_{P\text{-}e}$ and $\Delta R_{P\text{-}e}(0)$ will have a small effect on the deduced $r_{P\text{-}e}$. It is possible that the rapid relaxation of outer leaflet phospholipids very near a spin-label is lost during the shuttling time, so that only the relaxation of inner leaflet phospholipids is observed. However, we do not observe distinct biphasic behavior in the T_1 experiment as would be expected if phospholipid in both leaflets had dramatically different R_1 behavior. The $\Delta R_{P\text{-}e}(0)$ values extrapolated from this analysis and the distances are summarized in Table 1. Estimates of the error in $r_{P\text{-}e}$ for the different spin-labeled proteins were obtained by using a 2-μs $\tau_{P\text{-}e}$ (based on fitting the PC relaxation by spin-labeled D205C) and the maximum and minimum of $\Delta R_{P\text{-}e}(0)$ using that value to fit residual relaxation effects.

The distances from many of the spin-labeled sites to the substrate analogue PMe are consistent with this phospholipid binding to the enzyme active site. The largest effects are from a spin-label on W47C, part of helix B, which is thought to insert into the bilayer above the active site opening (9, 13), and H82C, the general acid in the catalytic mechanism for PI cleavage (14). However, there are some spin-labeled sites that were expected to have an effect but were fairly ineffective, notably attached to Y118C and N243C, both of which are close to the active site in the crystal structure.

The distances from the various spin-labels to the activator PC map to a very different site. The PC phosphorus is closest to the spin-label on D205C, whereas spin-labels at W47C, H82C, and N243C are slightly further away. These residues are at the rim of the $\alpha\beta$-barrel. In particular, Trp^{47} in helix B and Asn^{243} in a flexible rim loop are in regions shown to be important in membrane binding (9, 13).

Short Chain PC Sites on PI-PLC—To obtain further evidence for a discrete activator binding site, we examined the PRE

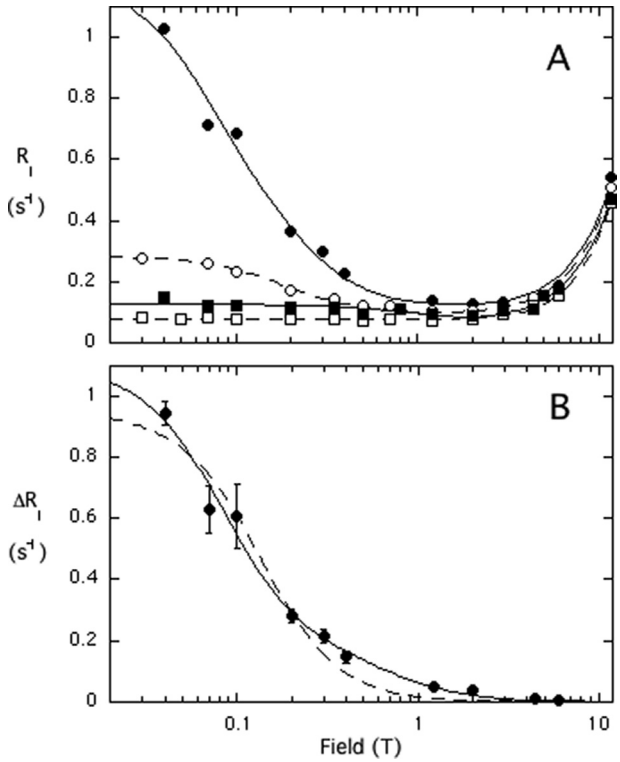

FIGURE 3. *A*, effect of 14.4 μM spin-labeled D205C (*filled symbols*) or H82C (*open symbols*) on the relaxation of 5 mM diC$_4$PC (■, □) or 5 mM diC$_6$PC (●, ○). *B*, field dependence of the additional diC$_6$PC R_1 component due to spin-labeled D205C fit with a single correlation time (*dashed line*) or two correlation times (*solid line*). *Error bars* are as defined in Fig. 2.

effects of spin-labeled D205C and H82C (14.4 μM) on two short chain phosphatidylcholines at lipid concentrations (5 mM) where they are monomeric in the absence of protein (the critical micelle concentration for dibutyroyl-PC (diC$_4$PC) is > 150 mM and that for dihexanoyl-PC (diC$_6$PC) is 14 mM (15)). Neither spin-labeled protein has much of a PRE effect on the diC$_4$PC molecules (Fig. 3*A*), although there is a very small effect from labeled D205C (see supplement and Fig. S3). In contrast, both spin-labeled proteins contributed to the relaxation of the longer chain lipid diC$_6$PC, with D205C having a much larger effect. This suggests that the lack of effect of the spin-labeled proteins on the shorter chain diC$_4$PC is because hydrophilic PC does not bind well to the distinct site on the protein.

As described above, the spin-label-induced PRE of diC$_6$PC can be fit to extract $\tau_{P\text{-}e}$ and $\Delta R_{P\text{-}e}(0)$ and ultimately distance. However, unlike phospholipids in vesicles, the PI-PLC·diC$_6$PC complex has overlapping dispersions requiring two discrete correlation times, one in the 10-ns range (τ_f) and a second in the 100-ns range (τ_s) (Fig. 3*B* and Table 2). Details of this convolution are shown in the supplement with the deconvolution shown in Fig. S2. The value of τ_s is larger than would be expected for a 35-kDa protein binding a small molecule, suggesting that the diC$_6$PC is forming a micellar aggregate with the protein. As observed with the vesicles, there appears to be a discrete PC binding site that is closer to the spin-label attached to D205C than to H82C (Table 2). Note that the different behavior with respect to the two spin-labeled proteins rules out nonspecific effects on loosely bound "micellar" diC$_6$PC.

Importantly, the distances between the spin-labels and diC_6PC ^{31}P are similar to the values obtained for PC in vesicles: 12.7 *versus* 13.5 Å for D205C and 15.7 *versus* 16.4 Å for H82C. These observations strongly indicate that PC binds to a discrete effector site on PI-PLC with a k_{off} similar to that for the substrate analogue leaving the active site.

Comparison of Phosphocholine Docking on PI-PLC with NMR Estimates of $r_{P\text{-}e}$ for PC—AutoDock4 was used to identify potential effector binding sites on PI-PLC for a phosphocholine headgroup. This program uses the crystal structure of the protein and does not allow significant conformational changes of the protein. However, it is useful to see whether there is a site with predicted affinity for a phosphocholine moiety. If a site is suggested, a comparison of distances in this model to the distances estimated with field-cycling and spin-labeled PI-PLC can provide evidence for conformational changes of the protein in its membrane-bound conformation.

Although diC_4PC does not bind well to the protein (inferred from Fig. 3*A*), we used butylphosphocholine as the ligand in the docking studies because the binding of a molecule containing a longer alkyl chain would be driven by hydrophobic effects of the chain rather than the headgroup. This should be a reasonable approach to looking for sites, because, for a PC molecule in a vesicle, the headgroup is the likely moiety that is recognized and bound by the protein with the rest of the aggregate providing hydrophobic interactions for the acyl chains. Fig. 4 shows a representative conformation of the butylphosphocholine docked to the monomer protein (Protein Data Bank code 1PTD). All of the low energy complexes populated the same region of the protein with the phosphocholine moiety. The same site also was identified when butylphosphocholine was docked to a PI-PLC dimer (see supplemental Fig. S4) that had been suggested to occur on membranes (16, 17). The PC site suggested in these docking experiments is ~15 Å from the substrate binding site. Occupation of this binding site would orient longer acyl chains of a PC molecule so they would stick into the membrane. The model orients the choline-$N(CH_3)_3^+$ near several surface tyrosine side chains (most notably Tyr^{204}, Tyr^{247}, and Tyr^{251}). Replacement of several of these tyrosines with serine dramatically reduces both PC activation (16) and the association of PI-PLC with PC-containing vesicles (18).

The distances predicted by the AutoDock model (measured from the Cα to the P atom) are generally in good agreement with those estimated from the field-cycling experiments (Fig. 4*C*), given the mobility of both the spin-label and the protein. One outlier is the spin-label at Y118C. The relaxation experiments indicate that the spin-label is much closer to PC than predicted from the structure and much farther from PMe at the active site. Tyr^{118} is very close to the active site, so it is possible that this modification perturbs

TABLE 2

τ and $\Delta R(0)$ parameters and distance, $r_{P\text{-}e}$, of the diC_6PC ^{31}P to spin-label sites of D205C and H82C extrapolated from the slower correlation time

Parameter	D205C	H82C
τ_f (ns)	13.0 ± 9.1	6.8 ± 1.3
$\Delta R_f(0)$ (s^{-1})	0.17 ± 0.07	0.040 ± 0.005
τ_s (ns)	112 ± 11	65.1 ± 3.3
$\Delta R_s(0)$ (s^{-1})	0.93 ± 0.07	0.15 ± 0.01
$r_{P\text{-}e}$ (Å)	12.7 ± 0.2[a]	15.7 ± 0.1[a]

[a] Both τ_s and $\Delta R_s(0)$ could be obtained in the fit for both samples (5 mM diC_6PC and 14.4 μM protein), with slightly larger errors in τ_s. Therefore, the maximum and minimum τ_s were used to find the range in $r_{P\text{-}e}$ (and hence the error).

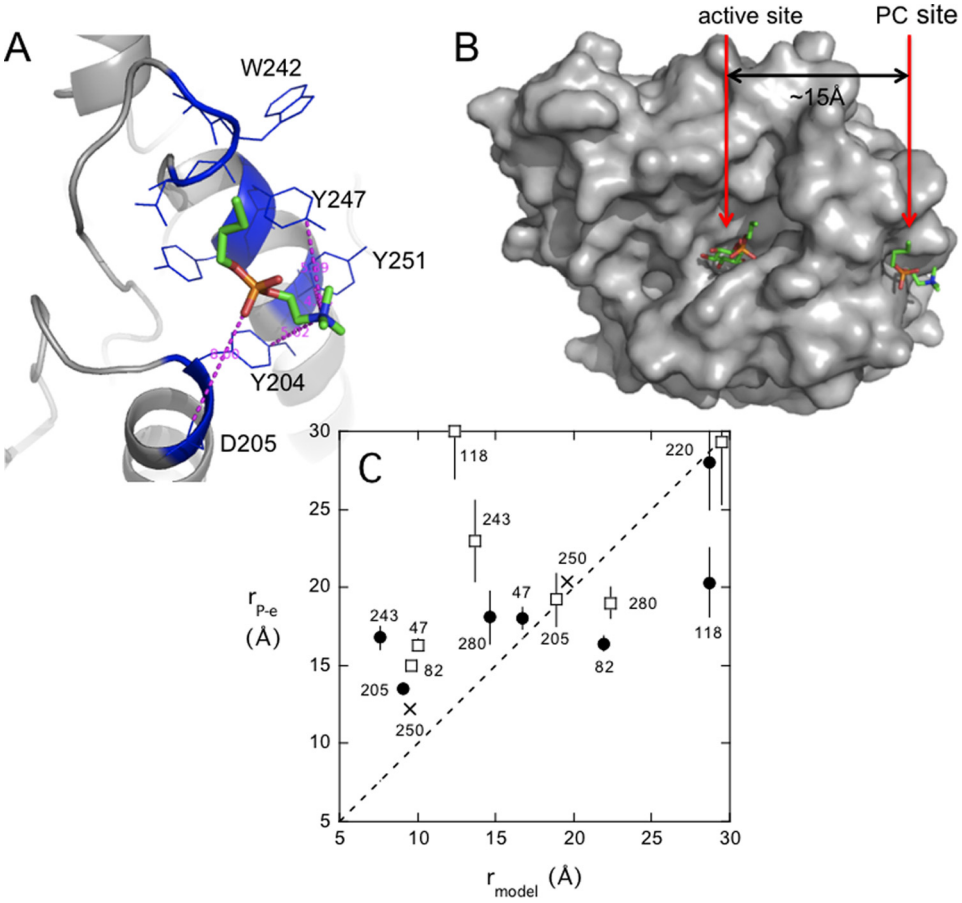

FIGURE 4. **AutoDock4 model for the butylphosphocholine binding site on PI-PLC.** *A*, energy-minimized structure around the activator binding site showing PC analogue interactions with nearby side chains. *B*, *top view*, looking down from the membrane at the spatial relationship of the novel PC binding site occupied by butylphosphocholine (*PC*) to the active site with a butylphosphoinositol bound (aligned with myoinositol in crystal structures of Protein Data Bank code 1PTG). The butyl tail of both small molecules is *green*. *C*, comparison of the distance estimated between the spin-label on a specific residue (indicated by a *number on the graph*) and ^{31}P of PC (●) or PMe (□) and the distance from the AutoDock model measured between the Cα of a specific residue on PI-PLC and the phosphorus atom of butylphosphocholine or phosphoinositol. The *diagonal line* shows the result for identical distances (or $y = x$). The two *X labels on the graph* are for spin-labeled S250C effects on PMe and PC as a test of the model. The *error bars* for $r_{P\text{-}e}$ are estimated as described in Table 2.

the structure and function of PI-PLC such that PMe no longer binds very tightly (although the specific activity of this mutant protein with mM substrate is within a factor of two of unmodified PI-PLC). If the lifetime of the bound lipid at this site was <0.2 μs, it is unlikely we would see much of an effect on R_1 at low fields. The stronger than expected effect on PC may indicate that this altered PI-PLC contains more than one binding site for PC. Future studies will examine the effect of spin-labels on this region of the protein coupled with detailed binding studies (18).

The distances measured for spin-labeled N243C to both PMe and PC also are significantly longer than predicted from the modeling. This residue is found in the flexible rim loop containing Trp^{242}, which is critical for binding to membranes (9). The field-cycling results for both PMe and PC strongly suggest that the orientation of this loop changes when the protein is bound to vesicles.

To further confirm the location of the activator site, we examined the PRE effect of spin-labeled S250C on PC/PMe SUVs (Fig. 5). This side chain points away from the nearby tyrosines that are thought to interact with PC but is in the general region. Spin-labeled S250C has small effects on the relaxation of PMe (Fig. 5*A*); the field dependence of ΔR_1 can be fit to Equation 2 with $\tau_{P\text{-}e} = 1.6 \pm 0.7$ μs and $\Delta R_{P\text{-}e}(0) = 1.16 \pm 0.44$ s^{-1}. This translates to a P-e distance of 20.4 $\pm$ 1.4Å, in good agreement with what is predicted from the protein structure. (The ^{31}P of phosphoinositol to the Cα of Ser^{250} is estimated as 19.6 Å in the model.)

In contrast, the presence of spin-labeled S250C has dramatic effects on the relaxation of PC (Fig. 5*B*). The value of R_1 increases as field decreases down to 0.015 T as the presence of the spin-label increases relaxation but appears to decrease at lower fields, perhaps because the relaxation of the outer leaflet lipids becomes too fast to measure. Fig. 5*C* shows ΔR_1 at fields $\geq$0.015 T. Fitting these data to Equations 1 and 2 with $\tau_{P\text{-}e} = 2$ μs (the value for most of the other vesicles) yields $\Delta R_{P\text{-}e}(0) = 33 \pm 6\ s^{-1}$ and $r_{P\text{-}e} = 12.2 \pm 0.4$ Å. If, instead, we used $\tau_{P\text{-}e} = 1.6$ μs from fitting the data for PMe in this system, the reduced $\Delta R_{P\text{-}e}(0)$ leads to a very similar ^{31}PC to spin-label distance of 12.5 $\pm$ 0.4 Å. Thus, the S250C spin-label to the PC ^{31}P distance is consistent with the discrete activator site suggested by modeling.

Conclusions—In summary, the high resolution field-cycling experiments demonstrate the following. (i) Specific enzyme-bound lipid complexes must exist while the protein is anchored on the membrane, and these have a lifetime of >2 μs (a time considerably shorter than that for overall dissociation of the protein from the vesicle). (ii) The substrate binding site is spatially separated ($\sim$15 Å) from the activator site. And, (iii) the loop with Asn^{243} (and a key tryptophan whose interaction with membranes is thought to be important) is likely to adopt a conformation that removes it from the vicinity of the headgroups of both discrete phospholipid binding sites.

A key advantage of the high resolution field-cycling PRE methodology is that far less enzyme is needed to see a spin-labeled enhancement of ^{31}P relaxation at very low fields as compared with measuring line width changes at high field, the more conventional approach, for the same system. For the latter, considerably more protein per phospholipid (typically $>$1:50) is needed to get an accurate change if one is starting with phospholipid line widths of 50–70 Hz.[5] At that high relative concentration of protein, the external surface of the vesicles is nearly covered with protein (5), so that more nonspecific effects of spin-labeled protein also may be occurring. Determining the correlation time for the spin-labeled relaxation of the phospholipid also is easier and considerably more accurate with the high resolution field-cycling method.

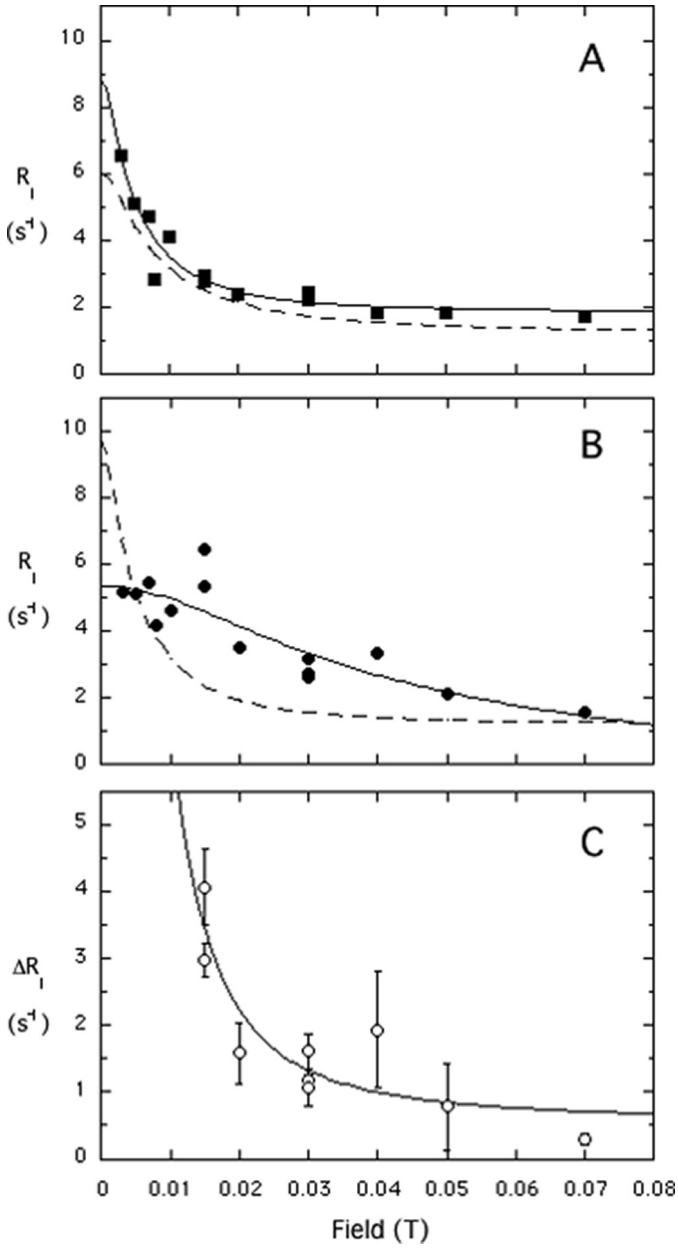

FIGURE 5. Shown is the low field dependence of the ^{31}P R_1 of 5 mM PMe (*A*) and 5 mM PC (*B*) in SUVs with 0.014 mM spin-labeled S250C present. The *dashed lines* represent R_1 for each phospholipid with the same concentration of unlabeled PI-PLC present. In *C*, the difference in R_1 for PC down to 0.015 T is shown. The *solid line* shows the fit with $\tau_{P\text{-}e} = 2$ μs. *Error bars* in *C* are defined in Fig. 2.

The novel method illustrated here with PI-PLC may be extended to a wide range of proteins that reversibly bind to

[5] M. Pu and M. F. Roberts, unpublished results.

membranes. Though the monitoring of ^{31}P nuclei restricts the system to small multicomponent vesicles, monitoring of ^{13}C-carbonyl-labeled phospholipids (19) would enable the use of large unilamellar vesicles and more biologically complex membranes. The methodology also should be applicable to non-lipid problems where ligands (large or small but containing ^{31}P (20), or ^{13}C without directly bonded protons (19)) in fast exchange with large complexes can be used to map out distances to specific spin-labeled probes on the macromolecule.

Acknowledgment—We thank Dr. Lizbeth Hedstrom (Department of Biology, Brandeis University) for critical comments on the manuscript.

REFERENCES

1. Heinz, D. W., Ryan, M., Bullock, T. L., and Griffith, O. H. (1995) *EMBO J.* **14,** 3855–3863
2. Zhou, C., and Roberts, M. F. (1998) *Biochemistry* **37,** 16430–16439
3. Zhou, C., Wu, Y., and Roberts, M. F. (1997) *Biochemistry* **36,** 347–355
4. Zhou, C., Qian, X., and Roberts, M. F. (1997) *Biochemistry* **36,** 10089–10097
5. Pu, M., Fang, X., Redfield, A. G., Gershenson, A., and Roberts, M. F. (2009) *J. Biol. Chem.* **284,** 16099–16107
6. Roberts, M. F., and Redfield, A. G. (2004) *J. Am. Chem. Soc.* **126,** 13765–13777
7. Roberts, M. F., and Redfield, A. G. (2004) *Proc. Natl. Acad. Sci. U.S.A.* **101,** 17066–17071
8. Redfield, A. G. (2003) *Magn. Reson. Chem.* **41,** 753–768
9. Feng, J., Wehbi, H., and Roberts, M. F. (2002) *J. Biol. Chem.* **277,** 19867–19875
10. Victor, K., Van-Quynh, A., and Bryant, R. G. (2005) *Biophys. J.* **88,** 443–454
11. Huey, R., Morris, G. M., Olson, A. J., and Goodsell, D. S. (2007) *J. Comput. Chem.* **28,** 1145–1152
12. Morris, G. M., Huey, R., Lindstrom, W., Sanner, M. F., Belew, R. K., Goodsell, D. S., and Olson, A. J. (2009) *J. Comput. Chem.* **30,** 2785–2791
13. Guo, S., Zhang, X., Seaton, B. A., and Roberts, M. F. (2008) *Biochemistry* **47,** 4201–4210
14. Hondal, R. J., Zhao, Z., Kravchuk, A. V., Liao, H., Riddle, S. R., Yue, X., Bruzik, K. S., and Tsai, M. D. (1998) *Biochemistry* **37,** 4568–4580
15. Bian, J., and Roberts, M. F. (1992) *J. Colloid. Interface Sci.* **153,** 420–428
16. Shi, X., Shao, C., Zhang, X., Zambonelli, C., Redfield, A. G., Head, J. F., Seaton, B. A., and Roberts, M. F. (2009) *J. Biol. Chem.* **284,** 15607–15618
17. Shao, C., Shi, X., Wehbi, H., Zambonelli, C., Head, J. F., Seaton, B. A., and Roberts, M. F. (2007) *J. Biol. Chem.* **282,** 9228–9235
18. Pu, M., Roberts, M. F., and Gershenson, A. (2009) *Biochemistry* **48,** 6835–6845
19. Sivanandam, V. N., Cai, J., Redfield, A. G., and Roberts, M. F. (2009) *J. Am. Chem. Soc.* **131,** 3420–3421
20. Pu, M., Feng, J., Redfield, A. G., and Roberts, M. F. (2009) *Biochemistry* **48,** 8282–8284